PROTECTION AGAINST SOURCE INFERENCE ATTACKS IN FEDERATED LEARNING

Anonymous authors
Paper under double-blind review

ABSTRACT

Federated learning (FL) was initially proposed as a privacy-preserving machine learning paradigm. However, FL has been shown to be susceptible to a series of privacy attacks. Recently, there has been concern about the *source inference attack* (SIA), where an honest-but-curious central server attempts to identify exactly which client owns a given data point which was used in the training phase. Alarmingly, standard gradient obfuscation techniques with differential privacy have been shown to be ineffective against SIAs, at least without severely diminishing the accuracy.

In this work, we propose a defense against SIAs within the widely studied shuffle model of FL, where an honest shuffler acts as an intermediary between the clients and the server. First, we demonstrate that standard naive shuffling alone is insufficient to prevent SIAs. To effectively defend against SIAs, shuffling needs to be applied at a more granular level; we propose a novel combination of parameter-level shuffling with the *residue number system* (RNS). Our approach provides robust protection against SIAs without affecting the accuracy of the joint model and can be seamlessly integrated into other privacy protection mechanisms.

We conduct experiments on a series of models and datasets, confirming that standard shuffling approaches fail to prevent SIAs and that, in contrast, our proposed method reduces the attack's accuracy to the level of random guessing.

1 INTRODUCTION

Federated learning (FL) (55) is a machine learning scheme that trains a global model across multiple clients without centralizing their data. The clients first update the model using their local datasets and then send the model updates to a central server, which aggregates them to form the global model W. The most well-known aggregation function is *FedAvg*, where $W \leftarrow \frac{1}{n}\sum_{i=1}^{n} w_i$, for n clients, each holding a local model w_i.

The initial concept of FL was that it was private by design, as the data of each client was not shared with anyone. Unfortunately, an honest-but-curious central server can launch a series of privacy attacks, as it observes the clients' reported model updates and can use them to infer information. For instance, the server can launch a *membership inference attack* (MIA) (58; 7; 11) which aims to determine if a particular data point exists in the training dataset of *any* client.

The *source inference attack* (SIA) (34; 35) has recently been proposed as a natural extension of the MIA. In an SIA, the adversary (an honest-but-curious central server) tries to determine *exactly which* client owns a given data point. To achieve this, the attacker compares the accuracy of the target data point across the received models before they are aggregated into the global model. This can pose a severe violation of privacy; consider for example a medical model jointly built by different hospitals to treat some disease and suppose that a hospital A is specialized in cancer cases. If the central server learns from a successful SIA that a patient's data was used by Hospital A, then they can confidently assume that the patient suffers from cancer.

Defending against SIAs While MIAs exploit model overfitting, SIAs work by exploiting differences in model predictions across clients due to their heterogeneous data distributions. Model obfuscation techniques such as differential privacy (DP) (22; 1) have been shown to be inadequate to protect against SIAs, at least without severely deteriorating the accuracy of the joint model (34; 35).

That is because the level of noise is required to be large to successfully make the different local models indistinguishable from each other.

Another approach is to consider regularization-based defenses, which can be beneficial against MIAs since they reduce overfitting (40). However, such defenses are insufficient for SIAs as they do not focus on reducing the distributional differences between clients (35). To verify, we include an empirical evaluation on all common regularization-based defenses (Appendix F). Our results show that regularization-based defenses have virtually no impact against SIAs.

Using defenses against Data Reconstruction Attacks (DRAs) (e.g. Instahide (37), FedAdOb (29)) are also ineffective as they focus on preventing gradient inversion. In contrast, SIAs assume that the attacker already knows that a given data point was used in training. We empirically verify that such defenses have no effect in Appendix F. Finally, (35) investigated whether knowledge distillation techniques (e.g. FedMD) can be a means of defense. FedMD was only able to slightly decrease the SIA success rate; the attack remains well above random guessing.

In this work, we focus on the shuffle model, which assumes the presence of a trusted shuffler. This approach, which provides additional privacy protection by permuting clients' data, has been widely studied in FL. Interestingly, although standard naive shuffling removes the connection between the data owner and their value, this is not enough to protect against SIAs. To show this, we propose a series of attacks aimed at defeating the effect of shuffling by remapping the values back to their original owners (Section 5).

Therefore, a new defense strategy against SIAs is necessary. We aim to satisfy these specifications:

- **S.1: Protection**: The accuracy of SIAs is reduced to the level of random guessing, even in the challenging scenario where clients hold datasets with a high level of dissimilarity.
- **S.2: Integrability**: The solution can be seamlessly integrated as a "module" into existing shuffle-model FL architectures, and is compatible with other privacy mechanisms, such as DP, which protect from other kinds of privacy attacks.
- **S.3: Communication efficiency**: Considering that SIAs are better suited for the cross-silo setting of FL (cf. Section 4) an increase in the communication cost can be tolerated, as long as it remains reasonable.
- **S.4: Maintains model accuracy**: DP does not protect against SIAs unless we pay a high price in accuracy. Hence, typical approaches based on DP-SGD would not be optimal.
- **S.5: Minimal trust assumptions**: Each client does not have to trust any additional entity.

Contributions Our contributions are summarized as follows:

- We propose novel *reconstruction attacks* that defeat standard shuffling in FL by remapping the shuffled values back to their original owners. We examine three shuffling methods; model-level, layer-level and parameter-level, and provide a corresponding reconstruction algorithm for each. These attacks enable SIAs within the standard shuffle model of FL, making shuffling alone insufficient (Section 5).
- We propose the first robust defense against SIAs in the shuffle model of FL. Our approach introduces a novel dimension-based shuffling method with higher granularity, using the *residue number system* (RNS). The defense reduces attack accuracy to random guessing without affecting joint model accuracy and can be seamlessly integrated into existing shuffle mechanisms (Section 6).
- We conduct experiments on the MNIST and CIFAR-10 with CNN and CIFAR-100 with ResNet-18 which validate our analyses (Section 7).

2 Related Work

FL remains vulnerable to various attacks despite the fact that raw data are not disclosed (68; 24; 34; 35). In (34; 35) the authors introduced the concept of SIAs and empirically showed, by performing experiments across a variety of datasets, that model overfitting and data distribution (increased heterogeneity) are the most important factors for making a model susceptible to SIAs.

Shuffling has been widely explored in the literature as a means to protect privacy. A shuffler can be implemented distributively using *trusted hardware* (5; 60), *multi-party computation* (51; 2; 50), *MixNets* (19; 8; 45; 33; 59), which can also be verifiable (43; 42) and *DC networks* (13; 12). In other words, the shuffler does not necessarily need to be a single separate server; its functionality could be performed distributively for instance even by the clients themselves (cf. Section 4).

In DP, the shuffle model was first introduced by (5) and later formalized in (9). This model has been applied in FL in a variety of ways to amplify the privacy by adding an additional layer of anonymity (61; 64; 27; 65; 49; 36; 46). Each user perturbs their model updates, then sends them to the shuffler which randomly permutates them before releasing them to the central server.

As far as we are aware of, no defense for SIAs has been studied in the literature, which is the motivation for this work. We have previously presented a preliminary shuffle-based approach to defending against SIAs in a poster (3) (*anonymized for reviewing*), which was effective but practically unfeasible due to its high communication cost.

3 PRELIMINARIES

Source inference attacks (SIAs) (34; 35) The adversary (central server) knows that a training record $z = (x, y)$ (where x is an input vector and y is a class label) is present in the training dataset. The source status of each record can be represented by an n-th dimensional multinomial vector s (where n is the number of clients). Only one element of $s_{i,j}$ is equal to 1 (indicating that client i owns the j-th record) and the others are set to 0. For the j-th record z_j, the source inference attack can be defined as follows:

Definition 1 (Source inference attack) *(34; 35) Given an local optimized model w_i and a training record z_j, source inference aims to infer the posterior probability of z_j belonging to the client i:*

$$\mathcal{S}(w_i, z_j) := P(s_{i,j} = 1 \mid w_i, z_j)$$

Encoding Schemes In this work, we combine shuffling with the following encoding schemes:

Definition 2 (Unary encoding) *If $x, k \in \mathbb{N}, x \leq k$, then x is encoded as:*

$$\mathcal{U}(x, k) = \{1\}^x \cup \{0\}^{k-x}$$

Moreover, we employ the residue number system (RNS) (23):

Definition 3 (RNS encoding) *If $m_1, m_2, \ldots, m_u$ are pairwise coprime, then $x \in \mathbb{N}$ is encoded as $\{x_1, x_2, \ldots, x_u\}$ where $x_i = x \bmod m_i$.*

Given the residues $x_1, x_2, \ldots x_u$, one can reconstruct x using the *Chinese remainder theorem* (we show an example in Appendix C.1). Also, Definition 3 can be extended for $x \in \mathbb{Z}$. If $x < 0$, the encoding is first performed for $|x|$, getting the resulting residues $x_1, x_2, \ldots x_u$. Then, x is encoded as $\{m_1 - x_1, m_2 - x_2, \ldots, m_u - x_u\}$. Furthermore, the addition of two RNS encoded numbers can be performed directly in the RNS domain by summing their residues. Finally, the range of the RNS encoding is defined by the choice of the moduli:

Proposition 3.1 *$x \in \left[-\lfloor \frac{M}{2} \rfloor, \lfloor \frac{M-1}{2} \rfloor\right] \cap \mathbb{Z}$ can be losslessly encoded in the RNS, where $M = \prod_i m_i$.*

4 SETTING

In this section we clarify the setting on which we will focus and define the attacker.

Cross-Silo setting SIAs were proposed for the so-called *cross-silo* setting of FL, where the number of clients is limited (typically 2-100 clients (39)) but each has superior communication/computation capabilities. For instance, it can be hospitals cooperating to produce a joint model for some disease. This model is widely applied in real-world scenarios, ranging from medical data (31; 28; 56; 63; 53; 62; 15; 16) to the agricultural domain (21; 18; 32). The opposite setting, known as *cross-device*,

involves a larger number of clients, each with limited communication and computational capabilities. For example, it can be smart watches training a health-monitoring model.

Studying SIAs for the cross-silo setting is more natural, as the attack relies on the fact that each client has a specific attribute linked to its data points. In other words, a sensitive attribute that the adversary infers upon identifying which client trained a given data point. For example, a hospital is typically associated with the medical conditions it specializes in, making it likely that its patients suffer from a respective disease. Therefore, in this work, we focus on the cross-silo setting, in line with previous research on SIAs (34; 35).

In previous works (34; 35), SIAs focused on supervised learning for classification tasks, as we do as well. We also assume that model parameters are clipped in $(-1, 1)$; this can be achieved by clipping and properly scaling them. Finally, we focus on the FedAvg aggregation function, but our approach can be generalized to any sum-based aggregation function (cf. Section 8).

Shuffle Model We assume a shuffle model architecture (e.g. a mechanism from (46; 61; 64; 27; 65; 49; 36)) and our goal is to propose a defense mechanism which requires minimal modifications. To highlight the appealing trust assumption of the shuffle model we give an example implementation with MixNets. Using Onion Encryption (20) and Zero-Knowledge Proofs (ZKPs), Algorithm 8 requires that *only one* server in the MixNet be trusted; all the others can be malicious. If we require each FL client to run their own server in the MixNet (a reasonable design choice given their resources in the cross-silo setting), then each client only has to trust themselves and no other entity, which satisfies our design specification **S.5**.

Attacker We consider an honest-but-curious central server as an adversary who sees the output of a trusted shuffler (or at least partially trusted with MixNets, i.e. at least one server in the MixNet is assumed to be trusted). We assume that the shuffler does not collude with the adversary (e.g. using the aforementioned Algorithm 8). The attacker knows that a particular data point z was used in the training phase (e.g. from a MIA) and their goal is to find, using an SIA, the client who owns it.

If no other information is known to the adversary then the standard shuffle model is sufficient to protect against SIAs since shuffling breaks the link between the data owner and their value. However, assuming that the adversary does not know anything more about the target client is arguably a strong assumption. In this work, we consider that the attacker knows a small *shadow dataset* only of the target client. A shadow dataset S_x of a target user x is a dataset disjoint from the one that x actually uses for training, which however follows the same distribution. For instance, using once more the hospital example, if the attacker is a pharmaceutical company it might already know that some of its patients were treated by the target hospital. Note that a similar assumption is often made in other privacy attacks like the MIA (58; 7; 11). We clarify that this shadow dataset will only be used to reverse the shuffling (Section 5); SIAs do not rely on the shadow dataset at all (Definition 1).

5 Reconstruction Attacks against Shuffling

In this section we show how an attacker can remap a shuffled model back to its original owner x by using their shadow dataset S_x. We begin with model-level shuffling, the standard approach used in the shuffle model of FL. Then, as illustrated in Figure 5, we expand the granularity to include layer-level and parameter-level shuffling, showing that in all three cases reconstruction attacks are possible. The algorithms discussed in the following subsections are placed in the Appendix B.

5.1 Model-level Shuffling

The current widely-used approach in shuffle-based FL is shuffling at the level of model updates. In other words, the shuffler receives the model w_i from each user i, chooses a random permutation π and outputs $w_{\pi(1)}, \ldots, w_{\pi(n)}$. However, the adversary can defeat the shuffler by remapping the model back to the target client x, by comparing the accuracy of each model on the shadow dataset S_x (Algorithm 2). The model with the highest accuracy on S_x will, most probably, belong to client x. Observe that this attack is feasible for the adversary; if n is the number of clients and $||S_x||$ is the size of the shadow dataset, then Algorithm 2 has $O(n \cdot ||S_x||)$ complexity (as the adversary needs to find the accuracy on each of the samples of S_x on each of the clients).

5.2 LAYER-LEVEL SHUFFLING

Since standard (model-level) shuffling can be reversed, let us explore shuffling per layer of the neural network (46). For instance, if we consider a simple CNN with a convolutional layer $\mathcal{C}$ and 2 FC layers $FC1, FC2$, the shuffler releases: $\{\mathcal{C}_{\pi_0(1)}, \ldots, \mathcal{C}_{\pi_0(n)}, FC1_{\pi_1(1)}, \ldots, FC1_{\pi_1(n)}, FC2_{\pi_2(1)}, \ldots, FC2_{\pi_2(n)}\}$. In other words, for each FC and convolutional layer, the shuffler finds a *new* random permutation π. This does not affect the accuracy of the joint model because in FedAvg the order of the received layers is inconsequential.

Observe now that the adversary has to run Algorithm 2 on every possible combination of layers. Depending however on the model, the number of combinations can be significant, which might make this approach non-feasible. To counter this, we propose a strategy which focuses only on the final layer of the neural network (Algorithm 3). Assuming w.l.o.g. that this is a FC layer, say FC_L, the adversary focuses on correctly remapping each FC_L back to its original owner. For the remaining layers, the adversary computes their average (using FedAvg). This reduces the complexity again back to $O(n \cdot ||S_x||)$, for n clients. The intuition behind this approach is that the final layer of a model tends to contribute more to overfitting. As a result, it more strongly reflects the distributional differences of the inputs. This is precisely what SIAs exploit, enabling the adversary to focus on the final layer, which provides the greatest advantage.

5.3 PARAMETER-LEVEL SHUFFLING

Next, let us consider shuffling per dimension, i.e. for each parameter p of each layer the shuffler releases $p_{\pi(1)}, \ldots, p_{\pi(n)}$, an approach not yet explored in FL, as far as we are aware. Each random permutation π has to be resampled for each parameter p as otherwise the adversary could target the most easily distinguishable parameter (in case there are such outliers) to retrieve the permutation [1]. This approach does not affect the accuracy of the joint model; the central server can compute the aggregated model unimpeded.

This creates an obvious obstacle to the adversary: finding the best accuracy of each possible combination of parameters requires superior computational capabilities To overcome the hurdle, we follow a similar approach to Algorithm 3. That is, we once again focus only on reconstructing the final layer of the neural network (say FC_L with k parameters), taking the average of the other ones. However, now we first compute the average of FC_L and change each of its parameters p one by one. For each one, we select to keep the one out of the n choices (one from each client) that creates a model with the best accuracy on S_x. To summarize, we copy the global model; each time we change only one of its parameters from the final layer, examining the possible choices and storing the one with the highest accuracy (Algorithm 5), which has a complexity of $O(k \cdot n \cdot ||S_x||)$.

6 PROTECTION AGAINST SOURCE INFERENCE ATTACKS

While parameter-level shuffling presents the greatest challenge for an attacker to reconstruct, the attack still remains feasible especially for heterogeneous datasets, as we show experimentally in Section 7. In this section, we argue that to effectively defend against SIAs, parameter-level shuffling should be combined with encoding, which further enhances the granularity of shuffling.

To achieve robust protection, we increase the shuffling granularity to bits. We show that this ensures that only the aggregated result of each parameter is leaked to the central server (which is necessary to compute the joint model) and not any information about the individual models. First, we compress the values using the residue number system (RNS) and then encode them into bits, using unary encoding (Definition 2). An outline of the proposed method is presented below; it is described in detail in Algorithm 1, with an example shown in Figure 4.

Recall from Section 3 that RNS encodes an integer x by performing a modulo operation with several pairwise coprime integers (called *moduli*). Since RNS is designed for integers [2], we consider a scaling factor 10^r, known to both the clients and the server, where the *precision* r corresponds to the

[1] We assume clients send all parameters at once, with the shuffler applying distinct permutations using sufficient metadata. Alternatively, parameters can be sent individually, which increases communication rounds.

[2] Floating-point RNS (10) is not suitable as summing the values by their shuffled residues is not possible.

number of digits of the fractional part that will be transmitted. Thus, every parameter $p \in (-1, 1)$ becomes $\lfloor p \cdot 10^r \rfloor$ and is then encoded using RNS. Each residue is then unary encoded and submitted in a separate shuffling round. The server can find the sum of each residue and, using the Chinese remainder theorem, reconstruct the sum of each parameter (which would need to be descaled by 10^r).

Algorithm 1: `Parameter-level shuffling with RNS`

Input: n clients, precision r, a function $RNS_{enc}(\cdot)$ for RNS encoding and $RNS_{dec}(\cdot)$ for decoding, a function $\mathcal{U}(x, k)$ for unary encoding x in k bits
Output: w_{glob}, the joint model

Let $\mathcal{M} = \{m_1, m_2, \ldots, m_u\}$ be pairwise coprime integers where $\prod_{m \in \mathcal{M}} m < n(10^r - 1)$
Client-side (each client i with model w_i):
`// Encode each parameter in RNS`
for *each parameter p in w_i* **do**
  $\{p_1, p_2, \ldots p_u\} \leftarrow RNS_{enc}(\lfloor p \cdot 10^r \rfloor, \mathcal{M})$
  for *each residue p_i in $\{p_1, p_2, \ldots p_u\}$* **do**
    Send $\mathcal{U}(p_i, m_i)$ to the shuffler.

Shuffler:
for *each parameter p* **do**
  Concatenate all the received bit vectors to a vector $B_{p,j}$ for each residue j.
  Shuffle (bit-wise) each $B_{p,j}$ and send it to the central server.

Server-side:
Receive the permutated bit vectors B'_p for each parameter p.
for *each i-th parameter of w_{glob}* **do**
  `// Sum and decode the residues to get the average of each parameter`
  $y \leftarrow (\sum B'_{p,0}, \sum B'_{p,1}, \ldots, \sum B'_{p,u})_{RNS}$
  $w_{glob}[i] \leftarrow (RNS_{dec}(y, \mathcal{M})/10^r)/n$

Return w_{glob}

Meeting the required specifications Our main insight is that revealing a shuffled bit vector is privacy-wise equivalent to revealing its sum (Proposition A.1). In other words, we show that Algorithm 1 releases only the aggregated model, without revealing any information about the individual local models. Since SIAs work by evaluating the accuracy of the given data point on the individual local models, this reduces their application to random guess, as there are no distinct models to compare.

Formally, we show that Algorithm 1 satisfies design specification **S.1** (Protection), in Theorem 1:

Theorem 1 *Algorithm 1 reduces the accuracy of SIAs to the level of random guessing.*

The proof of the above theorem is in Appendix A.

Then, **S.2** (Integrability) is also respected since only encoding/decoding operations need to be added. Regarding the communication cost (**S.3**), assuming n clients, the moduli $m_1, m_2, \ldots, m_u$ should be picked such that $n \cdot v < \lfloor \frac{(M-1)}{2} \rfloor$ (Proposition 3.1) where $M = \prod_i m_i$ and $v = 10^r - 1$ (i.e. the largest integer with r digits). Therefore, assuming u moduli with m_u being the largest, the cost is $O(u \cdot m_u)$. The number of shuffling rounds can be kept reasonably small, as it will be equal to the number of moduli (Figure 11). In general, small values are usually used for the residues (m_i), hence each user has to send a small number of m_i bits in each round, keeping the communication cost reasonable, as we show in Section 7. Furthermore, **S.4** (Accuracy) is preserved with a sufficient r since RNS encoding is lossless (Claim A.1). Finally, our proposed solution does not require additional trust assumptions than the ones of the shuffle model. Our proposed defense is fully compatible with the example implementation of shuffling with MixNets (Algorithm 8), where each user only has to trust themselves, satisfying **S.5**.

In summary, the combination of RNS, unary encoding and parameter-level shuffling enables strong privacy without sacrificing much efficiency. We use Proposition A.1 to introduce a novel approach to

privacy amplification without adding any noise. By combining it with RNS, we can minimize the bit vectors and reduce communication cost. With this approach, we provide a novel noise-free yet optimal privacy protection, along with compression to limit efficiency loss.

Honest shuffler So far we have assumed an implementation where the shuffler is partially trusted, in the sense that we trust only one server in the MixNet (Section 4). However, the typical assumption in the literature of the shuffle model is that the shuffler is fully honest (27). In that case, Onion Encryption and Zero-Knowledge Proofs are not necessary thus the communication can be further optimized by coupling Algorithm 1 with compression techniques such as Run-Length Encoding (RLE); we describe the corresponding algorithm in Appendix B.2, which we further evaluate in Section 7.

6.1 Comparison with Secure Aggregation

One can view our approach as essentially turning the shuffler into a secure aggregator from the adversary's point of view by properly combining shuffling with encoding. Despite the fact that this work builds upon the shuffle model and a change in the architecture would violate the design specification **S.2**, a natural question arises about how our method compares with Secure Aggregation (SA) (6).

Applying threshold secret-sharing requires t out of n clients to reconstruct a secret, in order to minimize the cost and the risk of dropouts, where $t << n$ (e.g. $t = 0.5 \cdot n + 1$ (6)). Therefore, the protocol is private to any $t - 1$ malicious coalitions of clients. On the contrary, shuffling with MixNets requires only 1 out of n servers to be trusted (e.g. Algorithm 8). Thus, the two models need to be compared under a common denominator, which is a common trust assumption. This can be achieved by implementing SA with standard threshold secret-sharing with $t = n - 1$, aligning with the trust assumption of the shuffle model (and our design specification **S.5.**). Each user must send C bits to every other user, where C is the size of each share, increasing the communication cost to $C \cdot (n - 1)$. Now the liveness constraints become a significant problem since, even if one client drops out the secret cannot be recovered. In contrast, MixNets can still shuffle and release the output even if all but one server drops out. In conclusion, SA incurs a stronger trust assumption and liveness constraints; we compare nevertheless our approach with this setting in Section 7.

7 Evaluation

This section presents the primary experiments; additional evaluation can be found in Appendix F.

Setting For the SIAs we use the same code as (34; 35) in order to provide comparable results, which also includes the structures of the neural networks. We use a CNN for MNIST and CIFAR-10 and a ResNet-18 for CIFAR-100 (cf. Appendix D). The success rate of the attack is defined as the percentage of the correct guesses on the given data points. Training is performed across 20 rounds for MNIST and across 100 rounds for CIFAR-10 and CIFAR-100 but only the best SIA accuracy is reported. The number of local epochs is set to 10. As an upper baseline for the experiments we use the accuracy of the SIA when no shuffling is used (vanilla FL) and as a lower baseline the random guess (uniform over the clients). We split the dataset among the clients using the Dirichlet distribution with a parameter α (level of heterogeneity). Finally, we assume that the adversary has a shadow dataset of 5% the size of the target client's actual training dataset (in Appendix F.2 we repeat the experiments for 0.5% and 1% yielding similar conclusions).

7.1 Protection against SIAs

In this experiment, we test the SIA accuracy on the proposed Algorithm 1 and also on the Algorithms 2, 3 and 5 that remap the shuffled models back to their original owners from Section 5. Figure 1 shows the results relative to the level of heterogeneity (α).

Model-level shuffling is the least effective choice; Algorithm 2 can reliably reverse shuffling, particularly when α is small. Notably, SIAs demonstrate a high success rate on CIFAR-100 with ResNet-18, as the increased complexity of the dataset amplifies the differences between the generated local

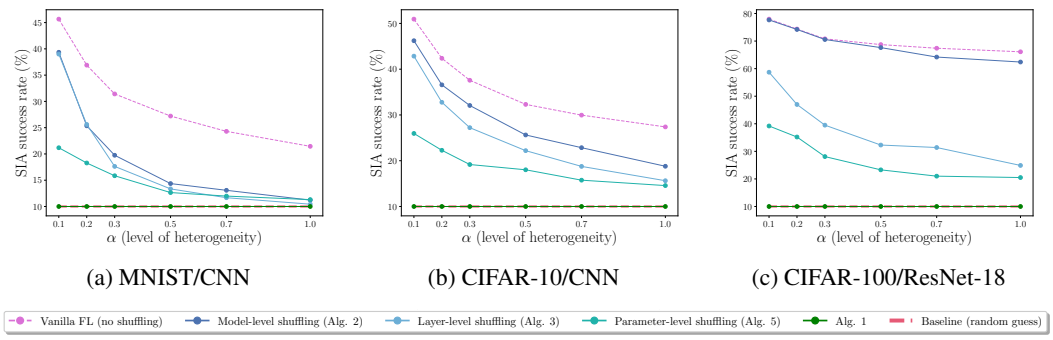

(a) MNIST/CNN (b) CIFAR-10/CNN (c) CIFAR-100/ResNet-18

Figure 1: Success rate of SIA for 10 clients

models. Layer-level shuffling exhibits slightly lower performance on MNIST and CIFAR-10 than Algorithm 2. On CIFAR-100, however, the difference is larger; for instance, Algorithm 2 achieves approximately $\approx 78\%$ accuracy, while Algorithm 3 reaches only $\approx 60\%$ for $\alpha = 0.1$. This larger gap may be explained by the increased complexity of the ResNet architecture, where overfitting may also be stored in layers other than the final one, which Algorithm 3 targets. Parameter-level shuffling is the best choice among the three. Algorithm 5 cannot reconstruct as well the shuffled models; the accuracy of the SIA is reduced, for instance from 50% to 28% on the CIFAR-10 for $\alpha = 0.1$. Still, however, the SIA accuracy remains higher than random guessing. Our proposed solution of Algorithm 1 offers robust protection in the sense that it always reduces the accuracy to the level of random guess, validating Theorem 1.

In conclusion, the experiment shows that a straightforward application of shuffling might not be enough to protect against SIAs, especially in scenarios with high heterogeneity which are arguably the most relevant cases for SIAs. In contrast, our proposed solution provides an optimal defense. We also evaluate with more clients and other aggregation functions, such as FedSGD and FedProx, as well as an MLP network, which are placed in Appendix F, since they lead to similar conclusions.

Protection against DRAs Although our main focus in this paper is on defending against SIAs, we also empirically demonstrate in Appendix F.3 that Algorithm 1 can also mitigate Data Reconstruction Attacks (DRAs). DRAs have been shown to depend heavily on the training batch size (67). By applying Algorithm 1, we shuffle the models at such a fine granularity that only the aggregated model is exposed, effectively simulating a larger batch size. For example, if the batch size is 1 with n clients, Algorithm 1 yields an aggregated model similar to having a single client train with a batch size of n. Specifically, while the reconstruction loss of the original DRA of (69) is $3 \cdot 10^{-4}$, it increases to 0.98 when Algorithm 1 is applied with 10 clients on the CIFAR-10 dataset. Consequently, the reconstructed images become heavily degraded, containing no recognizable features. We elaborate further in Appendix F.3, showing additional experiments.

7.2 Performance Analysis

Accuracy of the joint model Algorithm 1 only considers the first r digits of the fractional part of each parameter. In this experiment, we show that r can be kept reasonably small to minimize the communication cost while preserving the accuracy of the joint model. Figure 3 shows that for the MNIST, which requires a simpler model, $r = 2$ suffices to reach a level of accuracy comparable to vanilla FL and $r = 3$ scores a similar accuracy. On the other hand, CIFAR-10 and CIFAR-100, which require more complex models, need $r = 3$ digits to approach the performance of vanilla FL, and $r = 8$ to match it.

Communication Cost In Figure 2, we compare the communication cost of our approach against the baseline of vanilla FL (standard 32-bit binary encoding), which however transmits the whole value (whereas Algorithm 1 transmits only the first r digits). As an upper baseline we compare our approach with Secure Aggegation (SA), implemented with standard secret-sharing, with $t = n - 1$ (cf. Section 6.1), setting the smallest possible C to avoid overflows (for the first r digits). Moreover,

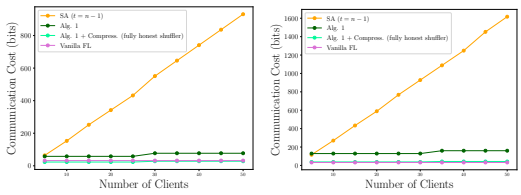

(a) $r = 4$ (b) $r = 8$

Figure 2: Communication Cost (bits per client per parameter).

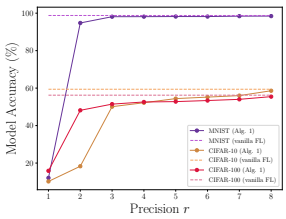

Figure 3: Model Accuracy (top-1) of Alg. 1 with precision r compared to vanilla FL (10 clients).

we evaluate the combination of Algorithm 1 with RLE compression which further reduces the communication cost, when the shuffler is fully honest (described in Appendix B.2).

For 10 clients and $r = 4$ the expansion factor, compared with vanilla FL, is $1.81\times$ on CIFAR-100/ResNet (Figure 13). This is an arguably manageable additional cost for the cross-silo setting, considering that the state-of-the-art protocol for SA for the cross-device setting exhibits an expansion factor of at least $1.73\times$ (6). Note that a direct comparison between the two is not meaningful as (6) relies on a stronger trust assumption (honest majority), as we explained in Section 6.1. Nevertheless, if an expansion of $1.73\times$ is deemed acceptable for the cross-device setting, a slightly higher factor should also be considered reasonable for the cross-silo setting, given the significantly superior communication capabilities of the clients. Finally, if we follow the literature of shuffle-model FL and assume a fully honest shuffler, then the expansion factor drops to $1.03\times$, approaching the cost of vanilla FL (Figure 13).

Table 5 shows that the proposed technique scales well as the number of clients and r increases (e.g. for more complex models). For example, even with 10^4 clients (a rather non-realistic scenario in the cross-silo setting which we consider) and $r = 16$, Algorithm 1 needs 440 bits per parameter (or 79 bits with compression under a fully trusted shuffler), compared to 32 bits for vanilla FL and ≈ 83 KBs of SA.

The computation cost of Algorithm 1 for encoding/decoding is negligible as it is based on primitive operations. For instance, the approximately 11 million parameters of ResNet can be encoded in 19 seconds; we further evaluate this in Appendix F.6.

8 Conclusion

In this work, we explored defenses against SIAs in FL by combining shuffling with encoding. Our proposed mechanism is easily integrable within the shuffle model of FL and fully compatible with other privacy protection mechanisms, such as DP, as its addition does not affect DP guarantees or further degrade accuracy. Moreover, we empirically showed that it also offers protection from DRAs. Another contribution of our work, potentially of independent interest, is the model reconstruction attacks to defeat a standard shuffler in datasets with a high level of dissimilarity. Future work should evaluate this attack on the state-of-the-art FL mechanisms of the shuffle model, as it has been shown that different mechanisms provide varying privacy guarantees when the shuffler is compromised (4).

In this work we focused on the shuffle model of FL. Developing similar defenses in settings where there is no shuffler remains an interesting step for future research. Moreover, we focused on FedAvg but our approach can be generalized to any other sum-based aggregation function, such as (48; 54; 57; 47; 25), where the central server sums the parameters and then performs further processing. To verify, we performed experiments on FedSGD and FedProx (Appendix F.4). Our work covers the vital class of sum-based aggregation functions which is widely used, for example in medical applications (63; 53; 62; 15; 16). We aim to further extend our approach to non sum-based frameworks, such as median-based, clustering-based and ranking-based (e.g. (66; 26; 38)).

Finally, we did not consider disaggregation attacks (52; 44), where the central server is given only the joint model and attempts to retrieve the local models. A possible direction for future work would be to pair disaggregation attacks with SIAs, as similar work has been done for attribute inference (41).

REFERENCES

[1] Martin Abadi, Andy Chu, Ian Goodfellow, H. Brendan McMahan, Ilya Mironov, Kunal Talwar, and Li Zhang. Deep learning with differential privacy. In *Proceedings of the 2016 ACM SIGSAC Conference on Computer and Communications Security*, CCS '16, page 308–318, New York, NY, USA, 2016. Association for Computing Machinery.

[2] Ittai Abraham, Benny Pinkas, and Avishay Yanai. Blinder – scalable, robust anonymous committed broadcast. In *Proceedings of the 2020 ACM SIGSAC Conference on Computer and Communications Security*, CCS '20, page 1233–1252, New York, NY, USA, 2020. Association for Computing Machinery.

[3] Anonymous. Anonymized title (anonymized for double-blind reviewing). Anonymous venue, 2024.

[4] Andreas Athanasiou, Konstantinos Chatzikokolakis, and Catuscia Palamidessi. Enhancing metric privacy with a shuffler. Privacy Enhancing Technologies Symposium, 2025.

[5] Andrea Bittau, Úlfar Erlingsson, Petros Maniatis, Ilya Mironov, Ananth Raghunathan, David Lie, Mitch Rudominer, Ushasree Kode, Julien Tinnes, and Bernhard Seefeld. Prochlo: Strong privacy for analytics in the crowd. In *Proceedings of the 26th Symposium on Operating Systems Principles*, SOSP '17, page 441–459, New York, NY, USA, 2017. Association for Computing Machinery.

[6] Keith Bonawitz, Vladimir Ivanov, Ben Kreuter, Antonio Marcedone, H. Brendan McMahan, Sarvar Patel, Daniel Ramage, Aaron Segal, and Karn Seth. Practical secure aggregation for privacy-preserving machine learning. In *Proceedings of the 2017 ACM SIGSAC Conference on Computer and Communications Security*, CCS '17, page 1175–1191, New York, NY, USA, 2017. Association for Computing Machinery.

[7] Nicholas Carlini, Steve Chien, Milad Nasr, Shuang Song, Andreas Terzis, and Florian Tramer. Membership inference attacks from first principles. In *2022 IEEE symposium on security and privacy (SP)*, pages 1897–1914. IEEE, 2022.

[8] Chen Chen, Daniele E. Asoni, David Barrera, George Danezis, and Adrain Perrig. Hornet: High-speed onion routing at the network layer. In *Proceedings of the 22nd ACM SIGSAC Conference on Computer and Communications Security*, CCS '15, page 1441–1454, New York, NY, USA, 2015. Association for Computing Machinery.

[9] A. Cheu, A. Smith, J. Ullman, D. Zeber, and M. Zhilyaev. Distributed differential privacy via shuffling. In *EUROCRYPT*. Springer, 2019.

[10] Jen-Shiun Chiang and Mi Lu. Floating-point numbers in residue number systems. *Computers Mathematics with Applications*, 22(10):127–140, 1991.

[11] Christopher A Choquette-Choo, Florian Tramer, Nicholas Carlini, and Nicolas Papernot. Label-only membership inference attacks. In *International conference on machine learning*, pages 1964–1974. PMLR, 2021.

[12] Henry Corrigan-Gibbs, Dan Boneh, and David Mazieres. Riposte: An Anonymous Messaging System Handling Millions of Users . In *2015 IEEE Symposium on Security and Privacy (SP)*, pages 321–338, Los Alamitos, CA, USA, May 2015. IEEE Computer Society.

[13] Henry Corrigan-Gibbs and Bryan Ford. Dissent: Accountable anonymous group messaging. pages 340–350, 10 2010.

[14] Thomas M. Cover and Joy A. Thomas. *Elements of Information Theory (Wiley Series in Telecommunications and Signal Processing)*. Wiley-Interscience, USA, 2006.

[15] Erfan Darzi, Nanna M. Sijtsema, and P. M. A. van Ooijen. A comparative study of federated learning methods for covid-19 detection. *Scientific Reports*, 14(1):3944, 2024.

[16] Ittai Dayan, Holger R. Roth, Aoxiao Zhong, Ahmed Harouni, Amilcare Gentili, Anas Z. Abidin, Andrew Liu, Anthony Beardsworth Costa, Bradford J. Wood, Chien-Sung Tsai, Chih-Hung Wang, Chun-Nan Hsu, C. K. Lee, Peiying Ruan, Daguang Xu, Dufan Wu, Eddie Huang, Felipe Campos Kitamura, Griffin Lacey, Gustavo César de Antônio Corradi, Gustavo Nino, Hao-Hsin Shin, Hirofumi Obinata, Hui Ren, Jason C. Crane, Jesse Tetreault, Jiahui Guan, John W. Garrett, Joshua D. Kaggie, Jung Gil Park, Keith Dreyer, Krishna Juluru, Kristopher Kersten, Marcio Aloisio Bezerra Cavalcanti Rockenbach, Marius George Linguraru, Masoom A. Haider, Meena AbdelMaseeh, Nicola Rieke, Pablo F. Damasceno, Pedro Mario Cruz e Silva, Pochuan Wang, Sheng Xu, Shuichi Kawano, Sira Sriswasdi, Soo Young Park, Thomas M. Grist, Varun Buch, Watsamon Jantarabenjakul, Weichung Wang, Won Young Tak, Xiang Li, Xihong Lin, Young Joon Kwon, Abood Quraini, Andrew Feng, Andrew N. Priest, Baris Turkbey, Benjamin Glicksberg, Bernardo Bizzo, Byung Seok Kim, Carlos Tor-Díez, Chia-Cheng Lee, Chia-Jung Hsu, Chin Lin, Chiu-Ling Lai, Christopher P. Hess, Colin Compas, Deepeksha Bhatia, Eric K. Oermann, Evan Leibovitz, Hisashi Sasaki, Hitoshi Mori, Isaac Yang, Jae Ho Sohn, Krishna Nand Keshava Murthy, Li-Chen Fu, Matheus Ribeiro Furtado de Mendonça, Mike Fralick, Min Kyu Kang, Mohammad Adil, Natalie Gangai, Peerapon Vateekul, Pierre Elnajjar, Sarah Hickman, Sharmila Majumdar, Shelley L. McLeod, Sheridan Reed, Stefan Gräf, Stephanie Harmon, Tatsuya Kodama, Thanyawee Puthanakit, Tony Mazzulli, Vitor Lima de Lavor, Yothin Rakvongthai, Yu Rim Lee, Yuhong Wen, Fiona J. Gilbert, Mona G. Flores, and Quanzheng Li. Federated learning for predicting clinical outcomes in patients with covid-19. *Nature Medicine*, 27(10):1735–1743, 2021.

[17] A. De Santis and G. Persiano. Zero-knowledge proofs of knowledge without interaction. In *Proceedings., 33rd Annual Symposium on Foundations of Computer Science*, pages 427–436, 1992.

[18] Rahool Dembani, Ioannis Karvelas, Nur Arifin Akbar, Stamatia Rizou, Domenico Tegolo, and Spyros Fountas. Agricultural data privacy and federated learning: A review of challenges and opportunities. *Computers and Electronics in Agriculture*, 232:110048, 2025.

[19] Roger Dingledine, Nick Mathewson, and Paul Syverson. Tor: The Second-Generation onion router. In *13th USENIX Security Symposium (USENIX Security 04)*, San Diego, CA, August 2004. USENIX Association.

[20] Roger Dingledine, Nick Mathewson, and Paul Syverson. Tor: the second-generation onion router. In *Proceedings of the 13th Conference on USENIX Security Symposium - Volume 13*, SSYM'04, page 21, USA, 2004. USENIX Association.

[21] Aiden Durrant, Milan Markovic, David Matthews, David May, Jessica Enright, and Georgios Leontidis. The role of cross-silo federated learning in facilitating data sharing in the agri-food sector. *Computers and Electronics in Agriculture*, 193:106648, 2022.

[22] Cynthia Dwork, Frank McSherry, Kobbi Nissim, and Adam Smith. Calibrating noise to sensitivity in private data analysis. volume Vol. 3876, pages 265–284, 01 2006.

[23] Harvey L. Garner. The residue number system. In *Papers Presented at the March 3-5, 1959, Western Joint Computer Conference*, IRE-AIEE-ACM '59 (Western), page 146–153, New York, NY, USA, 1959. Association for Computing Machinery.

[24] Jonas Geiping, Hartmut Bauermeister, Hannah Dröge, and Michael Moeller. Inverting gradients-how easy is it to break privacy in federated learning? *Advances in neural information processing systems*, 33:16937–16947, 2020.

[25] Avishek Ghosh, Jichan Chung, Dong Yin, and Kannan Ramchandran. An efficient framework for clustered federated learning. *Advances in neural information processing systems*, 33:19586–19597, 2020.

[26] Avishek Ghosh, Jichan Chung, Dong Yin, and Kannan Ramchandran. An efficient framework for clustered federated learning. *IEEE Transactions on Information Theory*, 68(12):8076–8091, 2022.

[27] Antonious M. Girgis, Deepesh Data, Suhas N. Diggavi, Peter Kairouz, and Ananda Theertha Suresh. Shuffled model of federated learning: Privacy, accuracy and communication trade-offs. *IEEE J. Sel. Areas Inf. Theory*, 2(1):464–478, 2021.

[28] Google Cloud. Kakao healthcare advances medical ai with federated learning on google cloud, 2023. Accessed: 2025-05-08.

[29] Hanlin Gu, Jiahuan Luo, Yan Kang, Yuan Yao, Gongxi Zhu, Bowen Li, Lixin Fan, and Qiang Yang. Fedadob: Privacy-preserving federated deep learning with adaptive obfuscation, 2024.

[30] Kaiming He, Xiangyu Zhang, Shaoqing Ren, and Jian Sun. Deep residual learning for image recognition. In *Proceedings of the IEEE conference on computer vision and pattern recognition*, pages 770–778, 2016.

[31] Wouter Heyndrickx, Lewis Mervin, Tobias Morawietz, Noé Sturm, Lukas Friedrich, Adam Zalewski, Anastasia Pentina, Lina Humbeck, Martijn Oldenhof, Ritsuya Niwayama, Peter Schmidtke, Nikolas Fechner, Jaak Simm, Adam Arany, Nicolas Drizard, Rama Jabal, Arina Afanasyeva, Regis Loeb, Shlok Verma, Simon Harnqvist, Matthew Holmes, Balazs Pejo, Maria Telenczuk, Nicholas Holway, Arne Dieckmann, Nicola Rieke, Friederike Zumsande, Djork-Arné Clevert, Michael Krug, Christopher Luscombe, Darren Green, Peter Ertl, Peter Antal, David Marcus, Nicolas Do Huu, Hideyoshi Fuji, Stephen Pickett, Gergely Acs, Eric Boniface, Bernd Beck, Yax Sun, Arnaud Gohier, Friedrich Rippmann, Ola Engkvist, Andreas H. Göller, Yves Moreau, Mathieu N. Galtier, Ansgar Schuffenhauer, and Hugo Ceulemans. Melloddy: Cross-pharma federated learning at unprecedented scale unlocks benefits in qsar without compromising proprietary information. *Journal of Chemical Information and Modeling*, 64(7):2331–2344, 2024. PMID: 37642660.

[32] V. Hiremani, R. M. Devadas, Preethi, R. Sapna, T. Sowmya, P. Gujjar, N. S. Rani, and K. R. Bhavya. Federated learning for crop yield prediction: A comprehensive review of techniques and applications. *MethodsX*, 14:103408, May 2025.

[33] Susan Hohenberger, Steven Myers, Rafael Pass, and abhi shelat. Anonize: A large-scale anonymous survey system. In *2014 IEEE Symposium on Security and Privacy*, pages 375–389, 2014.

[34] H. Hu, Z. Salcic, L. Sun, G. Dobbie, and X. Zhang. Source inference attacks in federated learning. In *ICDM*. IEEE, 2021.

[35] Hongsheng Hu, Xuyun Zhang, Zoran Salcic, Lichao Sun, Kim-Kwang Raymond Choo, and Gillian Dobbie. Source inference attacks: Beyond membership inference attacks in federated learning. *IEEE Trans. Dependable Secur. Comput.*, 21(4):3012–3029, July 2024.

[36] Chenxi Huang, Chaoyang Jiang, and Zhenghua Chen. Shuffled differentially private federated learning for time series data analytics. In *2023 IEEE 18th Conference on Industrial Electronics and Applications (ICIEA)*, pages 1023–1028, 2023.

[37] Yangsibo Huang, Zhao Song, Kai Li, and Sanjeev Arora. InstaHide: Instance-hiding schemes for private distributed learning. In Hal Daumé III and Aarti Singh, editors, *Proceedings of the 37th International Conference on Machine Learning*, volume 119 of *Proceedings of Machine Learning Research*, pages 4507–4518. PMLR, 13–18 Jul 2020.

[38] Saeed Iqbal, Adnan N Qureshi, Musaed Alhussein, Khursheed Aurangzeb, Atif Mahmood, and Saaidal Razalli Bin Azzuhri. Dynamic selectout and voting-based federated learning for enhanced medical image analysis. *Machine Learning: Science and Technology*, 6(1):015010, 2025.

[39] Peter Kairouz, H. Brendan McMahan, Brendan Avent, Aurélien Bellet, Mehdi Bennis, Arjun Nitin Bhagoji, Kallista A. Bonawitz, Zachary Charles, Graham Cormode, Rachel Cummings, Rafael G. L. D'Oliveira, Salim El Rouayheb, David Evans, Josh Gardner, Zachary Garrett, Adrià Gascón, Badih Ghazi, Phillip B. Gibbons, Marco Gruteser, Zaïd Harchaoui, Chaoyang He, Lie He, Zhouyuan Huo, Ben Hutchinson, Justin Hsu, Martin Jaggi, Tara Javidi, Gauri Joshi, Mikhail Khodak, Jakub Konečný, Aleksandra Korolova, Farinaz Koushanfar, Sanmi

Koyejo, Tancrède Lepoint, Yang Liu, Prateek Mittal, Mehryar Mohri, Richard Nock, Ayfer Özgür, Rasmus Pagh, Mariana Raykova, Hang Qi, Daniel Ramage, Ramesh Raskar, Dawn Song, Weikang Song, Sebastian U. Stich, Ziteng Sun, Ananda Theertha Suresh, Florian Tramèr, Praneeth Vepakomma, Jianyu Wang, Li Xiong, Zheng Xu, Qiang Yang, Felix X. Yu, Han Yu, and Sen Zhao. Advances and open problems in federated learning. *CoRR*, abs/1912.04977, 2019.

[40] Yigitcan Kaya, Sanghyun Hong, and Tudor Dumitras. On the effectiveness of regularization against membership inference attacks, 2020.

[41] Raouf Kerkouche, Gergely Ács, and Mario Fritz. Client-specific property inference against secure aggregation in federated learning. In *Proceedings of the 22nd Workshop on Privacy in the Electronic Society*, WPES '23, page 45–60, New York, NY, USA, 2023. Association for Computing Machinery.

[42] Albert Kwon, Henry Corrigan-Gibbs, Srinivas Devadas, and Bryan Ford. Atom: Horizontally scaling strong anonymity. In *Proceedings of the 26th Symposium on Operating Systems Principles*, SOSP '17, page 406–422, New York, NY, USA, 2017. Association for Computing Machinery.

[43] Albert Kwon, David Lazar, Srinivas Devadas, and Bryan Ford. Riffle: An efficient communication system with strong anonymity. *Proceedings on Privacy Enhancing Technologies*, 2016, 08 2015.

[44] Maximilian Lam, Gu-Yeon Wei, David Brooks, Vijay Janapa Reddi, and Michael Mitzenmacher. Gradient disaggregation: Breaking privacy in federated learning by reconstructing the user participant matrix, 06 2021.

[45] Simon Langowski, Sacha Servan-Schreiber, and Srinivas Devadas. Trellis: Robust and scalable metadata-private anonymous broadcast. 01 2023.

[46] Thomas Lebrun, Antoine Boutet, Jan Aalmoes, and Adrien Baud. Mixnn: protection of federated learning against inference attacks by mixing neural network layers. In *Proceedings of the 23rd ACM/IFIP International Middleware Conference*, Middleware '22, page 135–147, New York, NY, USA, 2022. Association for Computing Machinery.

[47] Daliang Li and Junpu Wang. Fedmd: Heterogenous federated learning via model distillation. *arXiv preprint arXiv:1910.03581*, 2019.

[48] Tian Li, Anit Kumar Sahu, Manzil Zaheer, Maziar Sanjabi, Ameet Talwalkar, and Virginia Smith. Federated optimization in heterogeneous networks. *Proceedings of Machine learning and systems*, 2:429–450, 2020.

[49] Ruixuan Liu, Yang Cao, Hong Chen, Ruoyang Guo, and Masatoshi Yoshikawa. Flame: Differentially private federated learning in the shuffle model. *Proceedings of the AAAI Conference on Artificial Intelligence*, 35(10):8688–8696, May 2021.

[50] Donghang Lu and Aniket Kate. RPM: Robust anonymity at scale. Cryptology ePrint Archive, Paper 2022/1037, 2022.

[51] Donghang Lu, Thomas Yurek, Samarth Kulshreshtha, Rahul Govind, Aniket Kate, and Andrew Miller. Honeybadgermpc and asynchromix: Practical asynchronous mpc and its application to anonymous communication. In *Proceedings of the 2019 ACM SIGSAC Conference on Computer and Communications Security*, CCS '19, page 887–903, New York, NY, USA, 2019. Association for Computing Machinery.

[52] Tanguy Marchand, Regis Loeb, Ulysse Marteau-Ferey, Jean Ogier Du Terrail, and Arthur Pignet. SRATTA: Sample re-ATTribution attack of secure aggregation in federated learning. In Andreas Krause, Emma Brunskill, Kyunghyun Cho, Barbara Engelhardt, Sivan Sabato, and Jonathan Scarlett, editors, *Proceedings of the 40th International Conference on Machine Learning*, volume 202 of *Proceedings of Machine Learning Research*, pages 23886–23914. PMLR, 23–29 Jul 2023.

[53] Pedro Mateus, Justine Moonen, Magdalena Beran, Eva Jaarsma, Sophie M van der Landen, Joost Heuvelink, Mahlet Birhanu, Alexander G J Harms, Esther Bron, Frank J Wolters, Davy Cats, Hailiang Mei, Julie Oomens, Willemijn Jansen, Miranda T Schram, Andre Dekker, and Inigo Bermejo. Data harmonization and federated learning for multi-cohort dementia research using the omop common data model: A netherlands consortium of dementia cohorts case study. *Journal of Biomedical Informatics*, 155:104661, 2024.

[54] Brendan McMahan, Eider Moore, Daniel Ramage, Seth Hampson, and Blaise Aguera y Arcas. Communication-efficient learning of deep networks from decentralized data. In *Artificial intelligence and statistics*, pages 1273–1282. PMLR, 2017.

[55] H. B. McMahan and E. et al. Moore. Communication-Efficient Learning of Deep Networks from Decentralized Data. In *AIST*. PMLR, 2017.

[56] Oasys Now. Oasys now - official website, 2025. Accessed: 2025-05-08.

[57] Sashank Reddi, Zachary Charles, Manzil Zaheer, Zachary Garrett, Keith Rush, Jakub Konečnỳ, Sanjiv Kumar, and H Brendan McMahan. Adaptive federated optimization. *arXiv preprint arXiv:2003.00295*, 2020.

[58] Congzheng Song Vitaly Shmatikov Reza Shokri, Marco Stronati. Membership inference attacks against machine learning models. In *2017 IEEE S&P*, pages 3–18, 2017.

[59] Krishna Sampigethaya and Radha Poovendran. A survey on mix networks and their secure applications. *Proceedings of the IEEE*, 94:2142 – 2181, 01 2007.

[60] Sajin Sasy, Aaron Johnson, and Ian Goldberg. Fast fully oblivious compaction and shuffling. In *Proceedings of the 2022 ACM SIGSAC Conference on Computer and Communications Security*, CCS '22, page 2565–2579, New York, NY, USA, 2022. Association for Computing Machinery.

[61] Lichao Sun, Jianwei Qian, and Xun Chen. Ldp-fl: Practical private aggregation in federated learning with local differential privacy. *arXiv preprint arXiv:2007.15789*, 2020.

[62] TNO. Federated learning: privacy-preserving data analysis, 2025. Accessed: 2025-09-23.

[63] Sebastian van der Voort. Federated learning in the healthcare setting, 2025. Accessed: 2025-09-23.

[64] Shuangqing Xu, Yifeng Zheng, and Zhongyun Hua. Camel: Communication-efficient and maliciously secure federated learning in the shuffle model of differential privacy, 2024.

[65] Qiantao Yang, Xuehui Du, Aodi Liu, Na Wang, Wenjuan Wang, and Xiangyu Wu. Adastopk: Adaptive federated shuffle model based on differential privacy. *Information Sciences*, 642:119186, 2023.

[66] Dong Yin, Yudong Chen, Ramchandran Kannan, and Peter Bartlett. Byzantine-robust distributed learning: Towards optimal statistical rates. In *International conference on machine learning*, pages 5650–5659. Pmlr, 2018.

[67] Hongxu Yin, Arun Mallya, Arash Vahdat, Jose M Alvarez, Jan Kautz, and Pavlo Molchanov. See through gradients: Image batch recovery via gradinversion. In *Proceedings of the IEEE/CVF conference on computer vision and pattern recognition*, pages 16337–16346, 2021.

[68] Ligeng Zhu, Zhijian Liu, and Song Han. *Deep leakage from gradients*. Curran Associates Inc., Red Hook, NY, USA, 2019.

[69] Ligeng Zhu, Zhijian Liu, and Song Han. Deep leakage from gradients. *Advances in neural information processing systems*, 32, 2019.

SUPPLEMENTARY MATERIAL

Ethics statement As discussed in Section 1, SIAs can pose a significant real-world privacy risk. Our proposed defense offers robust protection, making a positive contribution to user privacy. Notably, its ease of integration allows clients to implement the defense promptly. On the other hand, the proposed reconstruction attacks of Section 5 can undermine the privacy guarantees of shuffle-based FL mechanisms, thereby compromising the privacy of end users. Additional work is needed to verify their effectiveness across other shuffle-based mechanisms.

Reproducibility statement To make integration easier with current shuffle model mechanisms, we have implemented Algorithm 1 and placed its code in a public repository. For anonymity reasons, we do not include a link; yet the code can be found in the supplementary material. Using this same code, all experiments reported in the main body and appendix can be reproduced; a corresponding README file is included as guidance.

Use of LLMs We used Grammarly to fix awkward phrasing, grammatical errors and to improve the overall clarity of sentences.

APPENDIX

A PROOFS

In this section we include the missing proof of Theorem 1. We will use the notion of *Markov chain* in the information-theoretic sense (14). We recall that three random variables X, Y and Z form a Markov chain, denoted by $X \to Y \to Z$, if X and Z are conditionally independent given Y. Formally, $\forall x, y, z,\ P[Z = z|X = x, Y = y] = P[Z = z|Y = y]$, where P stands for probability.

We will also use other notions from information theory, namely *Shannon entropy* $H(X)$ and *conditional entropy* $H(X|Y)$, where X and Y are random variables. We recall that $H(X)$ represents the uncertainty about the value of X, and $H(X|Y)$ represents the remaining uncertainty about X after we learn Y.

First, we recall the well-known principle in information theory known as the *data processing inequality* (DPI), which states that *postprocessing* cannot increase the amount of information.

Theorem 2 *[Data processing inequality (14)] Let $X \to Y \to Z$ be a Markov chain. Then the Shannon conditional mutual entropy $H(\cdot|\cdot)$ satisfies the following property:*

$$H(X|Y) \leq H(X|Z).$$

Equality holds if and only if $X \to Z \to Y$ also is a Markov chain.

Since $H(X|Y)$ represents the remaining uncertainty about X after we learn Y, the above formula $H(X|Y) \leq H(X|Z)$ means that the amount of information that Y carries about X is less than the amount of information that Z (the result of postprocessing Y) carries about X.

We first prove that releasing a shuffled unary vector carries the same amount of information about the initial vector as releasing its sum:

Proposition A.1 *Let the random variable V range over vectors of bits of fixed length k, namely over $\{0,1\}^k$, let $S(V)$ represent the shuffling of V, and let ΣV represent the sum of all elements of V. Assume that the shuffler is a probabilistic function that depends only on the number of 1's in the vector. Then, the information that $S(V)$ carries about V is the same as the information that ΣV carries about V. Namely:*

$$H(V|S(V)) = H(V|\Sigma V).$$

Since the sum of the elements of V is the same as the sum of the elements of any shuffling of V, we have that V, $S(V)$ and ΣV form a Markov chain. Namely:

$$V \to S(V) \to \Sigma V$$

Therefore, by Theorem 2, we have:

$$H(V|S(V)) \leq H(V|\Sigma V) \tag{1}$$

On the other hand, since we are assuming that the result of the shuffling of V (i.e., the probability distribution over the shuffled vectors) depends only on the number of 1's in V, we have that also V, ΣV and $S(V)$ form a Markov chain:

$$V \to \Sigma V \to S(V)$$

From which we derive, applying again Theorem 2, that

$$H(V|\Sigma V) \leq H(V|S(V)). \tag{2}$$

Finally, from Equations (1) and (2), we can conclude.

We note that a related result, formulated in terms of probabilities, was shown in (9; 4) in the context of differential privacy.

Let us now prove the following property of Markov chains:

Proposition A.2 *Consider the following Markov chains:*

$$X \to Y \to Z \tag{3}$$

$$X \to Y \to W \tag{4}$$

where $Y = f(X)$ is a deterministic function.

If $H(Y|Z) = H(Y|W)$, then:

$$H(X|Z) = H(X|W).$$

From the first Markov chain in Equation (3), we deduce:

$$\begin{aligned} H(X|Z) &= H(X,Y|Z) && [X \to Y \text{ is deterministic}] \\ &= H(X|Y,Z) + H(Y|Z) && [\text{Chain rule}] \\ &= H(X|Y) + H(Y|Z) && [\text{Markov chain definition}] \end{aligned}$$

By applying the same reasoning to the second Markov chain in Equation (4), we obtain:

$$H(X|W) = H(X|Y) + H(Y|W).$$

Since $H(Y|Z) = H(Y|W)$, we conclude that $H(X|Z) = H(X|W)$.

Now we are ready to prove our main theorem about the protection of our mechanism.

Theorem 1 *Algorithm 1 reduces the accuracy of SIAs to the level of random guessing.*

We will show that Algorithm 1 reveals no more information than the aggregated result (i.e. the joint model), thereby reducing the SIA accuracy to that of a random guess by definition, as there are no distinct models to compare. We assume r is large enough so that the whole value is transmitted, which is the setting which leaks the most information.

Let X^j be the random variable ranging over the set of values that the users hold for some parameter j. Define for each residue m_u

$$\mathcal{Y}_u^j := \{x \bmod m_u : x \in X^j\}$$

and let Y_u^j be the corresponding random variable. The shuffler in Algorithm 1 receives the unary encoded values, concatenates them to a single vector and shuffles them altogether, outputting $S(\mathcal{Y})$ where

$$\mathcal{Y} := \bigcup_{y \in \mathcal{Y}_u^j} \mathcal{U}(y, m_u)$$

Let Y be the random variable that ranges over $\mathcal{Y}$. Note that Y depends only on Y_u^j. Hence the correlation between X^j, Y_u^j, and $S(Y)$ (the latter being the vector observed by the central server), can be described by the following Markov chain:

$$X^j \to Y_u^j \to S(Y) \tag{5}$$

Now, let us consider a scenario where the central server observes the aggregation (i.e., the summation) of Y_u^j, that we denote by ΣY_u^j, rather than its shuffled version. This is illustrated by the following Markov chain:

$$X^j \to Y_u^j \to \Sigma Y_u^j \tag{6}$$

Now note that $S(Y) = S(\bigcup \mathcal{U}(Y_u^j, m_u))$ (where $\bigcup \mathcal{U}(Y_u^j, m_u)$ represents the concatenation of the unary encoding of the elements of Y_u^j), and therefore Y_u^j, $S(Y)$ and ΣY_u^j satisfy the hypotheses of Proposition A.1, from which we derive

$$H(Y_u^j|S(Y)) = H(Y_u^j|\Sigma Y_u^j).$$

Given the avove equality, and Equations (5) and (6), we can apply Proposition A.2 and conclude that, for each parameter j and residue u:

$$H\big(X^j|S(Y)\big) = H\big(X^j|\Sigma Y_u^j\big).$$

The proof of Theorem 1 relied on the information which the central server first observes, since post-processing cannot increase the amount of information (*data processing inequality*).

However, recall that Algorithm 1 instructs the adversary to decode the result. Therefore, the adversary can still recover the aggregated model using RNS addition (Section 3). The only potential loss of information may arise from the parameter r (precision i.e. the digits transmitted after the decimal point). Since RNS encoding is lossless, we arrive at the following claim:

Claim A.1 *Assuming a sufficiently large r, Algorithm 1 does not impact the accuracy of the joint model.*

B ALGORITHMS

B.1 RECONSTRUCTION ATTACKS OF SECTION 5

We begin with Algorithm 2 which reverses model-level shuffling by remapping the models back to their original owners using the accuracy on the shadow dataset S_x of the target client x.

Then, for defeating layer-based shuffling, we assume w.l.o.g. 2 convolutional layers and 2 FC layers, presenting Algorithm 3. Note that for notational convenience, we use the FedAvg function to average layers (of neural networks) rather than entire models; the definition of the function remains similar.

Finally, Algorithm 5 shows a possible implementation of remapping parameter-level shuffling, assuming again w.l.o.g. 2 convolutional layers and 2 FC layers. Note that $\mathcal{FC}_{2,0}$ notates the shuffled set of the first parameters of the final FC layer $\mathcal{FC}_2$. Recall that each shuffle set has size n, if n is the number of clients. We assume that $\mathcal{FC}_2$ has k parameters.

Algorithm 2: $\mathcal{R}_{\mathcal{M}}$
Reconstruction attack against Model-level shuffling

Input : $w'_1, \ldots, w'_n$, randomly permutated clients' models,
S_x shadow dataset of target user x,
$A(w, D)$, accuracy of model w on the dataset D
Output : w_x, the model of user x
$best \leftarrow w'_1$
for *each model* w_j *in* $w'_2, \ldots, w'_n$ **do**
  if $A(w_j, S_x) > A(best, S_x)$ **then**
    $best \leftarrow w_j$
Return $best$

Algorithm 3: $\mathcal{R}_{\mathcal{L}}$
Reconstruction attack against Layer-level shuffling

Input : $\mathcal{C}_1, \mathcal{C}_2$, randomly permutated convolutional layers, $\mathcal{FC}_1, \mathcal{FC}_2$, randomly permutated FC layers,
S_x, shadow dataset of target user x,
$A(w, D)$, accuracy of model w on the dataset D
Output : w_x, a model with FC_2 of user x and the average of the rest layers
`// For FC2 find the one with best accuracy; take the FedAvg for the rest`
for *each layer* L_i *in* $\mathcal{FC}_2$ **do**
  $w \leftarrow CON(FedAvg(\mathcal{C}_1), FedAvg(\mathcal{C}_2), FedAvg(\mathcal{FC}_1), L_i)$
  Append w in w_{models}
Return $\mathcal{R}_{\mathcal{M}}(w_{models}, S_x, A)$

Algorithm 4: CON
Construct a model with given layers (used in Alg. 3)

Input : C_1, C_2, FC_1, FC_2 , layers of the model
Output : w, a model with the given layers
$w_{C1} \leftarrow C_1$
$w_{C2} \leftarrow C_2$
$w_{FC1} \leftarrow FC_1$
$w_{FC2} \leftarrow FC_2$
Return w

Algorithm 5: $\mathcal{R}_{\mathcal{P}}$
Reconstruction attack against Parameter-level shuffling

Input : w_{glob} , the global model
$\mathcal{FC}_{2,0}, \ldots, \mathcal{FC}_{2,k}$, randomly permutated parameters of the final layer
S_x, shadow dataset of target user x,
$A(w, D)$, accuracy of model w on the dataset D
Output : w_x, a model with FC_2 of user x and the average of the rest layers

$w_x \leftarrow w_{glob}$
for *each i-th set of parameters z_i in $\mathcal{FC}_{2,i}$* **do**
  $w_{best} \leftarrow REP(w_{glob}, i, z_{i,0})$
  $best \leftarrow z_{i,0}$
  for *each parameter j in z_i* **do**
    if $A(REP(w_{glob}, i, j), S_x) > A(w_{best}, S_x)$ **then**
      $w_{best} \leftarrow REP(w_{glob}, i, j)$
      $best \leftarrow j$
  $w_x \leftarrow REP(w_x, i, best)$
Return w_x

Algorithm 6: REP
Replace the i-th parameter of FC_2 with p (used in Alg. 5)

Input : w, a model
i, the $i-th$ parameter of FC_2
p, parameter to replace
Output : w', the output model

$w' \leftarrow w$
$w'_{FC_2}[i] \leftarrow p$
Return w'

B.2 Communication Improvement from Section 6

If we assume that the shuffler is fully honest, following the literature (27), then Onion Encryption is not necessary to hide the secrets (i.e. parameters) from the MixNet servers. Similarly, Zero-Knowledge Proofs are not required to verify that each server did not tamper with the data. In both cases, since the shuffler is honest, we assume it will follow the protocol and will not leak the secret values to an adversary. Thus, we can further improve the communication cost by adding a compression step after the unary encoding.

Run-Length Encoding (RLE) compresses a string by replacing consecutive repeated values with just a single value and a count of its repetitions. For example, AABAA will be represented as (2A,1B,2A). In our case we have bits; more specifically Unary Encoding (Definition 2) creates a bit-string by first placing the ones and then appending the zeroes. Since the size of the bit-string is known (i.e. r) we can send only the number of ones. For example, if we have $[1, 1, 1, 0, 0, 0, 0, 0, 0, 0]$ we can just send the number 3. The shuffler can create a bit-string with 3 ones and $r - 3 = 7$ zeroes. Algorithm 7 illustrates this idea.

C Example implementations

This section discusses an example of the Chinese remainder theorem and gives an example implementation of shuffling with MixNets. It also includes the figures that are missing from the main-body due to space constraints. Figure 5 shows the different shuffling granularities which we examined in Section 5 and Figure 4 illustrates a simple example of Algorithm 1.

C.1 Example of the Chinese Remainder Theorem

We show how the Chinese remainder theorem can be applied to reconstruct the secret value from the residues, using the example of Figure 4.

Algorithm 7: `Parameter-level shuffling with RNS combined with RLE`

Input: n clients, precision r, a function $RNS_{enc}(\cdot)$ for RNS encoding and $RNS_{dec}(\cdot)$ for decoding, a function $\mathcal{U}(x, k)$ for unary encoding x in k bits

Output: w_{glob}, the joint model

Let $\mathcal{M} = \{m_1, m_2, \ldots, m_u\}$ be pairwise coprime integers where $\prod_{m \in \mathcal{M}} m < n(10^r - 1)$

Client-side (each client i with model w_i):

`// Encode each parameter in RNS`

for *each parameter p in w_i* **do**

  $\{p_1, p_2, \ldots p_u\} \leftarrow RNS_{enc}(\lfloor p \cdot 10^r \rfloor, \mathcal{M})$

  for *each residue p_i in $\{p_1, p_2, \ldots p_u\}$* **do**

    Send p_i to the shuffler. `// Send the number of ones to the shuffler`

Shuffler:

for *each parameter p* **do**

  $\mathcal{B} \leftarrow \mathcal{U}(p_i, m_i)$ for each RNS moduli m_i and each received residue p_i. `// Decompress`

  Concatenate all the decompressed received bit vectors $\mathcal{B}$ to a vector $B_{p,j}$ for each residue j.

  Shuffle (bit-wise) each $B_{p,j}$ and send it to the central server.

Server-side:

Receive the permutated bit vectors B'_p for each parameter p.

for *each i-th parameter of w_{glob}* **do**

  `// Sum and decode the residues to get the average of each parameter`

  $y \leftarrow (\sum B'_{p,0}, \sum B'_{p,1}, \ldots, \sum B'_{p,u})_{RNS}$

  $w_{glob}[i] \leftarrow (RNS_{dec}(y, \mathcal{M})/10^r)/n$

Return w_{glob}

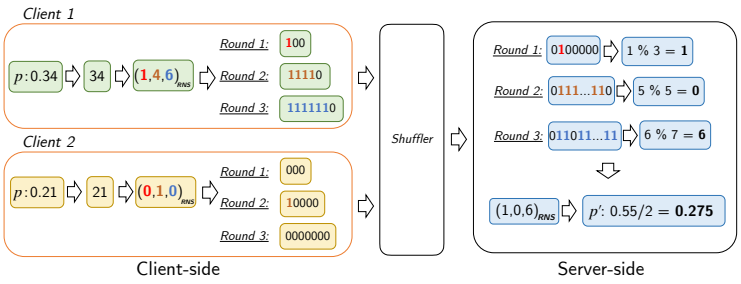

Figure 4: Example of Algorithm 1 with moduli $3, 5, 7$, for a parameter p, where $r = 2$ and $n = 2$.

Consider the following system of congruences, where $3, 5$, and 7 are pairwise coprime:

$$\begin{cases} x \equiv 1 \bmod 3 \\ x \equiv 0 \bmod 5 \\ x \equiv 6 \bmod 7 \end{cases}$$

We begin by computing the product of the moduli:

$$M = 3 \times 5 \times 7 = 105.$$

For each congruence, we define $M_i = M/m_i$, where m_i is the modulus of the i-th equation:

$$M_1 = 105/3 = 35, \quad M_2 = 105/5 = 21, \quad M_3 = 105/7 = 15.$$

Next, we compute the modular inverse y_i such that $M_i \cdot y_i \equiv 1 \bmod m_i$:

$$35 \cdot y_1 \equiv 1 \bmod 3 \Rightarrow y_1 = 2,$$

$$21 \cdot y_2 \equiv 1 \bmod 5 \Rightarrow y_2 = 1$$

$$15 \cdot y_3 \equiv 1 \bmod 7 \Rightarrow y_3 = 1.$$

We now apply the Chinese remainder theorem formula:

$$x \equiv a_1 M_1 y_1 + a_2 M_2 y_2 + a_3 M_3 y_3 \bmod M,$$

where $a_1 = 1, a_2 = 0, a_3 = 6$.

By substituting the values we have:

$$x \equiv 1 \cdot 35 \cdot 2 + 0 \cdot 21 \cdot 1 + 6 \cdot 15 \cdot 1 = 70 + 0 + 90 = 160 \bmod 105.$$

Thus, the solution is:

$$x \equiv 55 \bmod 105.$$

Observe that $x = 55$ indeed satisfies all original congruences:

$$55 \bmod 3 = 1, \quad 55 \bmod 5 = 0, \quad 55 \bmod 7 = 6.$$

C.2 SHUFFLING

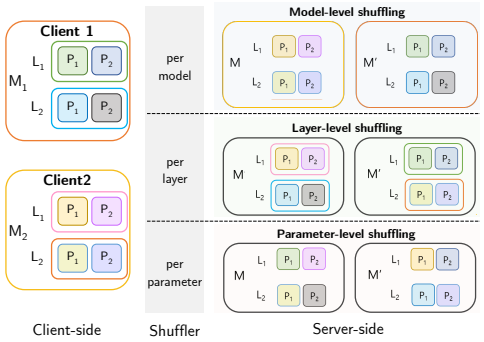

Figure 5: Shuffling methods in FL with different granularity

Algorithm 8 uses Onion Encryption (20) to ensure that no server can view the messages and Zero-Knowledge Proofs (ZKPs) (17) to assert that no server can change the messages. Each server decrypts the outermost layer of onion encryption, verifies that no tampering has occurred with a ZKP, shuffles and sends the shuffled vector to the next server. Since an honest shuffling (i.e. the fact that the previous server chose a uniformly random permutation) cannot be proved via ZKPs, at least one server of the MixNet needs to be trusted.

In scenarios where the clients cannot run their own MixNet server, they can instead choose more servers from the network to shuffle. For instance, they can decide to always select 100 servers out of all the available ones (a different set of servers for each parameter), meaning that the adversary must control all 100 servers to compromise the defense for each parameter. However, this requires an omnipotent adversary that controls a significant part of the MixNet network (even hacking honest servers like those run by the honest clients). This attacker is arguably unrealistic; often, anonymity systems, like Tor (20), assume that an attacker can only control parts of the network.

D MODELS AND HYPERPARAMETERS

This section describes the models which we used in the experiments of Section 7. For MNIST and CIFAR-10 we used exactly the same models as in (34; 35) [3], as we used their code for evaluating the SIAs. For CIFAR-100 we used the ResNet-18, in order to illustrate that the proposed mechanism works even on more complex models.

[3] https://github.com/HongshengHu/SIAs-Beyond_MIAs_in_Federated_Learning

Algorithm 8: Shuffling with MixNet

Input : M_i: Message client i wishes to send, n number of clients, P: List of participating mix servers, $\text{Onion}_{\text{Enc}}(M, \mathsf{pk})$ and $\text{Onion}_{\text{Dec}}(M, \mathsf{sk})$ for onion encryption/decryption
Output : Shuffled messages M'

```
// client-side
```
for *each client* i *in parallel* **do**
  $C_i \leftarrow M_i$
  `// onion-encryption`
  for *each mix server* j *in reverse order of* P **do**
    $C_i \leftarrow \text{Onion}_{\text{Enc}}(C_i, \mathsf{pk}_j)$
  Send C_i to P_1

```
// MixNet-side
```
for *each mix server* j *in* P **do**
  `// First server receives the messages (no ZKP to verify)`
  if $j = 1$ **then**
    $\mathbf{C} = [C_i]_{i=1}^{n}$
    $\pi \leftarrow$ None
  `// Last server outputs the messages`
  if $j = |P|$ **then**
    Return MixVerify($\mathbf{C}$, j, π).
  $\mathbf{C}, \pi \leftarrow$ MixVerify($\mathbf{C}$, j, π)

Algorithm 9: MixVerify(C,j,π)

Input : $\mathbf{C}$: Message from previous server, j: Current mix server, π_{j-1} ZKP from previous server, $\text{Verify}_{\text{ZKP}}(C, \pi)$ and $\text{Generate}_{\text{ZKP}}(\mathbf{C}, \mathbf{C}')$ to verify and generate ZKPs.
Output : Partially decrypted and shuffled message $\mathbf{C}'$

$M \leftarrow \text{Onion}_{\text{Dec}}(\mathbf{C}, \mathsf{sk_j})$
if $j > 1$ *and* $\neg$ *Verify*$_{ZKP}(M, \pi_{j-1})$ **then**
  reject and abort
$M' \leftarrow \text{Shuffle}(M)$
$\pi_j \leftarrow \text{Generate}_{\text{ZKP}}(M, M')$
Return M', π_j

D.1 MNIST

We use a CNN which consists of two convolutional layers with 5×5 kernels, followed by two max-pooling layers, and three fully connected layers. Specifically, the architecture is as follows:

- *Conv2D layer*: 32 filters with a kernel size of 5×5. Activation: *ReLU*. Input shape: *(1, 28, 28)*.
- *MaxPooling2D((2, 2))*.
- *Conv2D layer*: 64 filters with a kernel size of 5×5. Activation: *ReLU*.
- *MaxPooling2D((2, 2))*.
- *Flatten layer*: Flattens the feature maps into a 1D tensor of size $64 \times 4 \times 4$.
- *Dense layer*: 512 neurons. Activation: *ReLU*.
- *Dense layer*: 128 neurons. Activation: *ReLU*.
- *Output: Dense layer*: *1*0 neurons. Activation: *none (logits)*.

D.2 CIFAR-10

The CNN consists of two convolutional layers with 5×5 kernels (the first convolutional layer takes input images with three color channels (RGB)), followed by two max-pooling layers, and three fully connected layers. Specifically, the architecture is as follows:

- *Conv2D layer*: 32 filters with a kernel size of 5×5. Activation: *ReLU*. Input shape: *(3, 32, 32)*.
- *MaxPooling2D((2, 2))*.
- *Conv2D layer*: 64 filters with a kernel size of 5×5. Activation: *ReLU*.
- *MaxPooling2D((2, 2))*.
- *Flatten layer*: Flattens the feature maps into a 1D tensor of size $64 \times 5 \times 5$.
- *Dense layer*: 512 neurons. Activation: *ReLU*.
- *Dense layer*: 128 neurons. Activation: *ReLU*.
- *Output: Dense layer*: *1*0 neurons. Activation: *none (logits)*.

D.3 CIFAR-100

We use a standard ResNet-18 architecture (30) for CIFAR-100. Specifically, we use the implementation provided by the PyTorch library, initialized without pretrained weights (pretrained=False). The architecture is as follows:

- *Conv2D layer*: 64 filters with a kernel size of 7×7, stride 2, padding 3. Activation: *ReLU*. Input shape: *(3, 224, 224)*.
- *MaxPooling2D((3, 3))*, stride 2.
- *Residual Block (x2)*: Two convolutional layers with 64 filters, kernel size 3×3, batch normalization, and skip connections.
- *Residual Block (x2)*: Two convolutional layers with 128 filters. The first block includes downsampling via stride 2.
- *Residual Block (x2)*: Two convolutional layers with 256 filters. Includes downsampling.
- *Residual Block (x2)*: Two convolutional layers with 512 filters. Includes downsampling.
- *Global Average Pooling*: Output size reduced to a 512-dimensional vector.
- *Fully Connected Layer*: Output size 100 (number of classes). Activation: *none (logits)*.

D.4 Hyperparameters

For training, we used stochastic gradient descent (SGD) as the optimizer with a learning rate of 0.01 and a momentum of 0.9. Each client trained the model using a local batch size of 64, while the testing batch size was set to 128. These hyperparameters were selected following standard practice in FL literature and remained fixed across all experiments.

E Resources

To compute each point in Figure 1, Algorithm 2 and Algorithm 3 take approximately 1/2/7 hours for the MNIST/CIFAR-10/CIFAR-100 datasets, respectively. For the parameter reconstruction attack of Algorithm 5, the time required is approximately 20/40/70 hours for MNIST/CIFAR-10/CIFAR-100, respectively. Our proposed method (Algorithm 1) takes around 0.5/1/3 hours for MNIST/CIFAR-10/CIFAR-100, respectively, with nearly all of that time spent on training. We limit training to the first 10 epochs to reduce unnecessary computational cost, as SIA accuracy tends to be higher in early rounds when client models are more diverse. The experiments were conducted on a server equipped with two NVIDIA RTX 6000 GPUs (24 GB each), two AMD EPYC 7302 16-core processors, 512 GB of RAM, and 10 Gbps Ethernet connectivity.

The other experiments that do not necessitate the use of a GPU (i.e. Table 6 and Figure 2) were computed on a Mac M1 Laptop with a Apple Mac M1 Max chip and 64 GB of memory.

F Additional Evaluation

F.1 Other defenses against SIAs

(35) discusses that regulaziration-based defences are insufficient against SIAs. In this section we verify this claim by performing experiments on MNIST and CIFAR10 datasets with 10 clients and $\alpha = 0.1$ (the level of heterogeneity). Table 1 shows that all standard regularization approaches fail to address SIAs; rather, they may make the model even slightly more susceptible to them, as they might increase the distributional differences between clients.

Furthermore, we also test Instahide (37), which was designed for Data Reconstruction Attacks (DRAs). Instahide works by having each client blend their images with some k (a parameter of the mechanism) random, publicly accessible ones. This forms a layer of obfuscation which prohibits the adversary from reconstructing the images. Table 2 shows that this defense is ineffective against SIAs. Instahide focuses on preventing the adversary from reconstructing a particular image, but SIAs consider that the adversary does know that the image exists in the dataset. If the images are blended, with Instahide, then this means that the adversary already knows the blended image. Since this blend is not happening between clients (e.g. shuffling their images) but between each client and a public dataset, the distributional differences are not affected. Note that k in Instahide is small, meaning that only a small portion of the image is altered, to retain model accuracy.

Table 1: Regularization-based defenses against SIAs with 10 clients

Experiment	**Parameter**	**Dataset**	**Model Acc.**	**Model Acc. (vanilla FL)**	**SIA Acc.**	**SIA Acc. (vanilla FL)**
Random cropping	Crop=24	MNIST	92.56	97.22	50.24	45.01
	Crop=20	MNIST	83.30	97.22	53.17	45.01
	Crop=16	MNIST	62.15	97.22	56.10	45.01
	Crop=28	CIFAR10	58.78	61.07	52.50	51.57
	Crop=24	CIFAR10	53.66	61.07	53.07	51.57
	Crop=20	CIFAR10	44.81	61.07	59.20	51.57
Dropout	p=0.2	MNIST	96.45	97.22	55.70	45.01
	p=0.5	MNIST	96.28	97.22	50.92	45.01
	p=0.8	MNIST	96.42	97.22	45.17	45.01
	p=0.2	CIFAR10	60.76	61.07	57.77	51.57
	p=0.5	CIFAR10	60.38	61.07	55.20	51.57
	p=0.8	CIFAR10	60.52	61.07	54.54	51.57
Weight decay	e=0.5	MNIST	97.34	97.22	50.94	45.01
	e=0.4	MNIST	97.32	97.22	52.87	45.01
	e=0.3	MNIST	97.00	97.22	55.27	45.01
	e=0.5	CIFAR10	61.01	61.07	56.89	51.57
	e=0.4	CIFAR10	61.02	61.07	57.70	51.57
	e=0.3	CIFAR10	60.59	61.07	61.97	51.57

Table 2: Instahide against SIAs with $\alpha = 0.1$, 10 clients on the MNIST dataset. SIA accuracy on vanilla FL is 45.01% and vanilla model accuracy is 97.22%

k	Model Accuracy	SIA Accuracy
1	97.48	50.3
2	86.65	49.9
3	81.52	50.9
4	78.65	50.45
5	78.37	52.71

F.2 PROTECTION FROM SIAS

Figure 6 shows the success rate of SIA for Algorithm 1 and the reconstruction Algorithms 2, 3 and 5 with varying number of clients when α is fixed to 0.1 with 10 local epochs. We observe that the success rate depends on the number of clients which clarifies the reason why SIAs are more of a threat in the cross-silo setting. In all cases, model-level and layer-level shuffling offer insufficient protection, while parameter-level shuffling performs better but the SIA accuracy is still better than random guessing. In contrast our proposed method of Algorithm 1 offers robust protection.

Moreover, we conduct an experiment where we vary the number of local epochs (Figure 7), which does not yield notably different results because of the small α (i.e. datasets are already easily distinguishable).

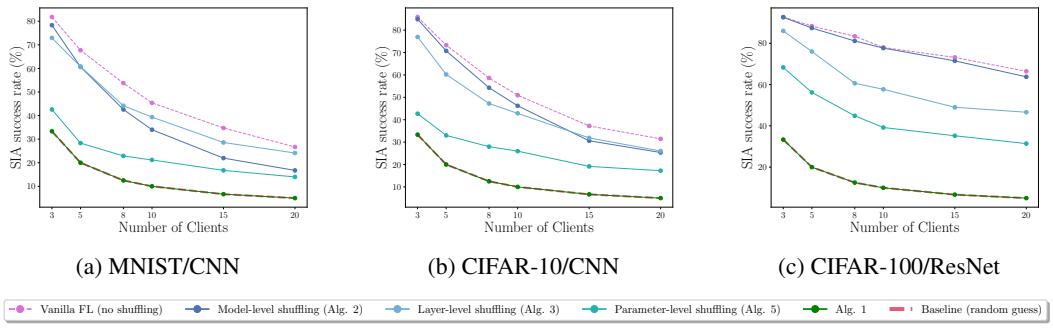

(a) MNIST/CNN (b) CIFAR-10/CNN (c) CIFAR-100/ResNet

Figure 6: Success rate of SIA for varying number of clients when $\alpha = 0.1$ with 10 local epochs

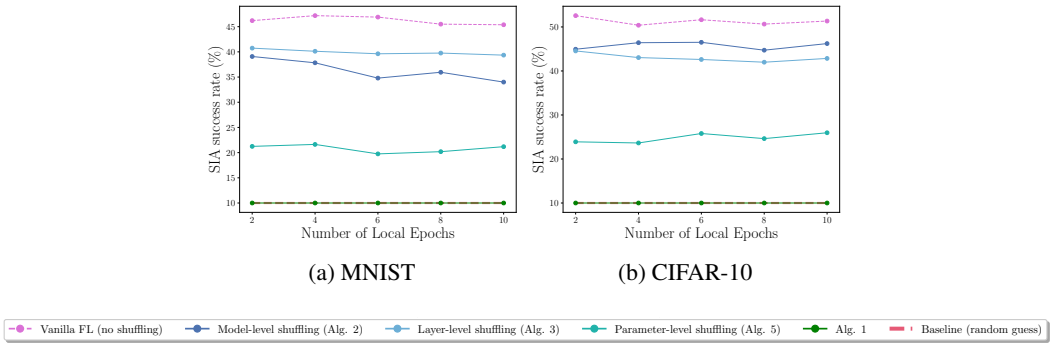

(a) MNIST (b) CIFAR-10

Figure 7: SIA success rate across different number of local epochs with 10 clients and $\alpha = 0.1$

Furthermore, we conduct experiments the Synthetic tabular dataset of (35), using the same MLP architecture as (35) for a fair comparison. Table 3 shows results consistent with the previous experiments, supporting the generality of SIAs. We observe that model-level, layer-level and parameter-level shuffling reduce the success rate of SIAs but fail to completely mitigate the attack. However, the proposed Algorithm 1 shows the same SIA accuracy as random guessing.

Table 3: SIA success rate on the synthetic dataset of (34) with MLP

Method	**Success Rate (%)**
Vanilla FL	46.2
Model-level shuffling (Alg. 2)	39.3
Layer-level shuffling (Alg. 3)	37.0
Parameter-level shuffling (Alg. 5)	21.1
Proposed Solution (Alg. 1)	10.0

In the experiments of the main body we assumed that the adversary holds a shadow dataset that is 5% of the one actually used. Table 4 shows that even when this percentage is smaller, the adversary still has an accuracy greater than random guessing (which is 10%).

Table 4: SIA success rate for a smaller shadow dataset (CIFAR-10/CNN, $n = 10$, $\alpha = 0.1$)

Method	**0.5% shadow db**	**1% shadow db**
Vanilla FL	51.57	51.57
Model-level shuffling (Alg. 2)	21.2	25.4
Layer-level shuffling (Alg. 3)	20.24	23.5
Parameter-level shuffling (Alg. 5)	16.2	19.1
Proposed Solution (Alg. 1)	10	10

F.3 Protection against Data Reconstruction Attacks

In this section we discuss how our proposed method can effectively defend against DRA. One of the earliest works on DRA, Deep Leakage from Gradients (DLG) (69), assumes that each client uses a very small batch size for local training (at most 8 samples). However, in our approach, all client gradients (or model parameters) are mixed before being transmitted to the server (using Algorithm 1). Thus, even if each client employs a batch size of 1, the aggregated gradient reflects n data points, where n is the number of clients.

We conducted experiments against the DLG attack of (69), which show that our approach can substantially reduce its effectiveness. Specifically, while the reconstruction loss of the original attack is 0.0003, it increases to 0.98 when Algorithm 1 is applied (even with as few as five clients). Thus the reconstructed images under Algorithm 1 become severely degraded, with no recognizable features Figure 8. Other DRA techniques are capable of operating with larger batch sizes (e.g., (67) employs up to 48 samples per client). However, (67) also shows that the success rate of the attack decreases as the batch size increases. This suggests that our method, by effectively conveying larger batch sizes, can further help mitigate DRA.

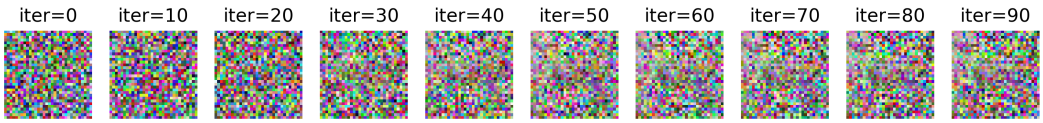

(a) 2 clients

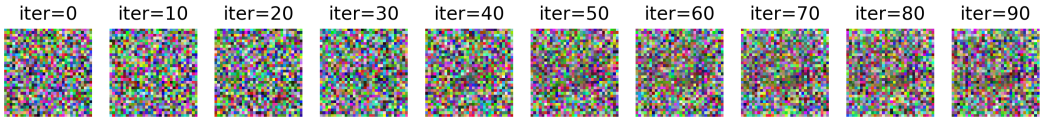

(b) 10 clients

Figure 8: DLG attack on Algorithm 1 (CIFAR-10 with batch size 1)

F.4 Other aggregation functions

Federated Proximal (FedProx) (48) adds a proximal term as a regularization penalty during local model optimization. The global model is then computed as the average of the local models. In Federated Stochastic Gradient Descent (FedSGD) (54) clients compute gradients over their data just once per round. The central server collects all local models and averages them.

Figure 9 shows that for both cases SIAs have higher success rate than random guessing for all standard shuffling approaches. In contrast, the proposed framework reduces the accuracy of the attacks to random guessing. This indicates that our approach can be extended to other sum-based aggregation

functions. Figure 10 shows that $r = 3$ suffices to reach an accuracy comparable to vanilla FL and $r = 5$ to match it.

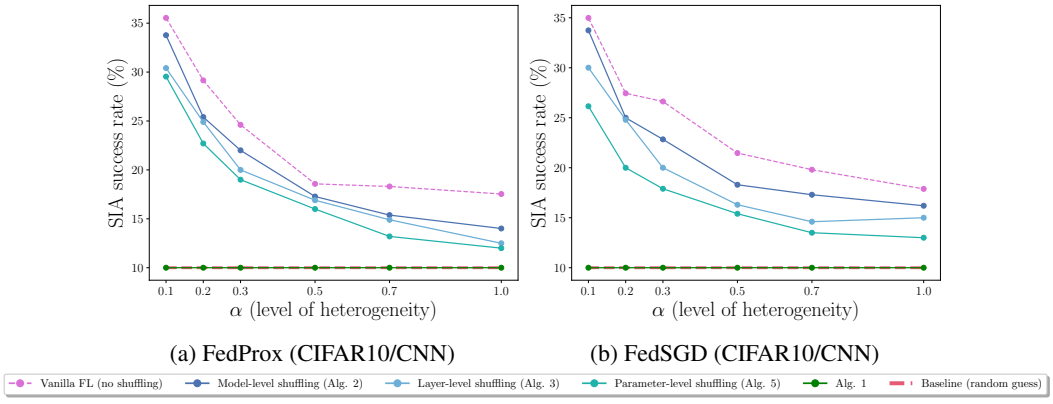

(a) FedProx (CIFAR10/CNN) (b) FedSGD (CIFAR10/CNN)

Figure 9: Success rate of SIA for 10 clients on FedProx and FedSGD

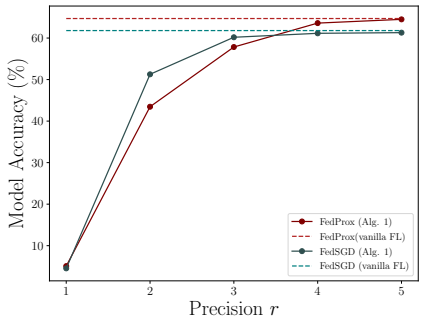

Figure 10: Model Accuracy (top-1) on CIFAR-10/CNN of Alg. 1 with precision r compared to vanilla FL (10 clients).

F.5 Communication Cost

Figure 11 shows that RNS can encode even large numbers using a small set of moduli, minimizing the number of shuffling rounds. Moreover, Figure 12 presents a zoomed-in view of Figure 2 for up to 20 clients. For $r = 4$, we observe that Algorithm 1 requires approximately 23 extra bits per parameter compared to vanilla FL, increasing to around 78 additional bits when $r = 8$. The communication cost of SA is slightly lower only when $r = 8$ and the number of clients is small (i.e. fewer than 5).

Note that Figure 12 shows that Alg. 1 with compression can even surpass standard vanilla FL. However, recall that Alg. 1 transmits only the first r digits of the parameter whereas vanilla FL transmits the whole value. Conversely, if one wants to use the standard binary compression of vanilla FL to transmit only the first r digits, they might be able to use less bits. For example if $r = 3$ than a 12-bit binary encoding is sufficient. In any case, we want to note that the proposed technique does not outperform vanilla FL in terms of communication cost, as it transmits less information.

Table 5 evaluates the proposed technique for more clients and more complex models (necessitating larger r). We observe that for both parameters Secure Aggregation scales poorly; in contrast the proposed technique offers reasonable communication cost, especially when combined with compression.

Finally, Figure 13 shows the expansion factor, that is the ratio of the encoded model size to the size of the initial vanilla FL model (i.e. using standard 32-bit binary encoding). The plot shows that for 10 clients, an expansion factor of $1.81\times$ is sufficient to achieve nearly the same accuracy as vanilla FL, and $2.4\times$ is needed to fully match it. If RLE compression is used, the expansion factor is $1.03\times$, which is a negligible overhead.

Table 5: Communication cost for larger parameters (bits per user per parameter)

Clients	r	SA	Alg. 1	Alg. 1 + Compress.	Vanilla FL
1000	8	36926	160	43	32
10000	8	399920	160	42	32
1000	12	49900	281	61	32
10000	12	539892	328	67	32
1000	16	63872	381	73	32
10000	16	669866	440	79	32

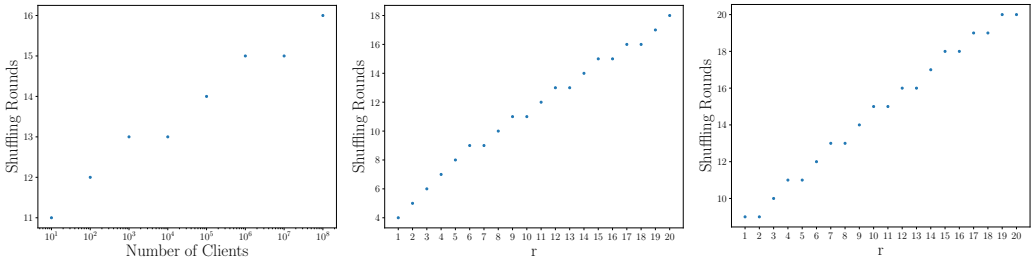

(a) $r = 10$ (b) 10 clients (c) 10^6 clients

Figure 11: Number of shuffling rounds in Algorithm 1

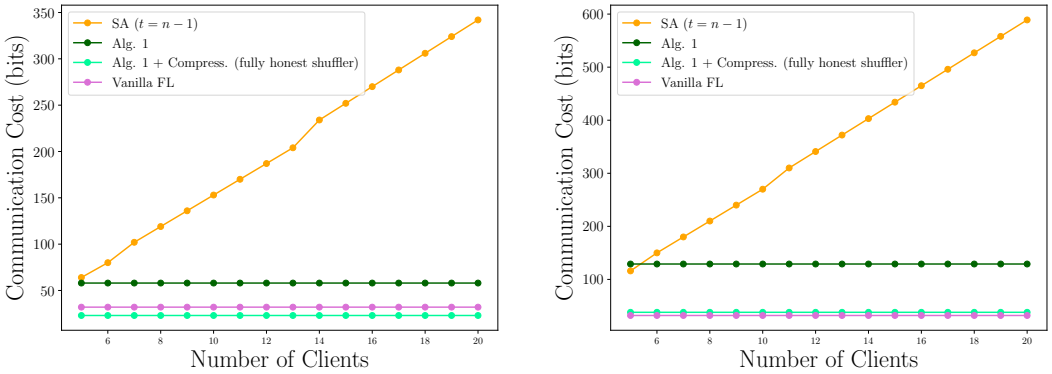

(a) $r = 4$ (b) $r = 8$

Figure 12: Communication Cost (bits per user per parameter).

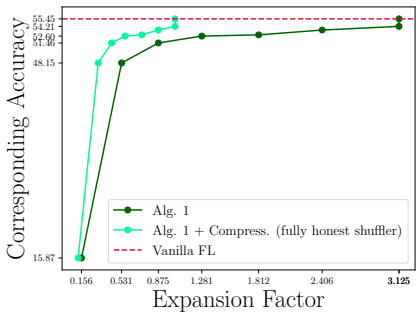

Figure 13: Expansion factor on CIFAR-100/ResNet when $n = 10$

F.6 Computation Cost

The encoding overhead of Algorithm 1 is negligible for the clients since it relies on fast and primitive operations (modulo and unary encoding). As shown in Table 6, even ResNet can be encoded in just 19.1 seconds, which is negligible compared to the total training time. Similarly, decoding (performed by the central server) is slightly slower but still remains efficient (e.g. slightly less than a minute for ResNet).

Table 6: Computation Time in seconds

DB/Model	**# of Parameters**	**Encoding**	**Decoding**
MNIST/CNN	643850	1.16	3.8
CIFAR-10/CNN	940362	1.6	5.6
CIFAR-100/ResNet	11237432	19.1	57

F.7 SIA Success Rate with subsampling

Figure 14 illustrates the accuracy of SIA when subsampling is applied. In the case of MNIST, the SIA accuracy drops significantly when the number of clients increases from 10 to 50 (from 45% to 10.2%), but rises again when client sampling is applied (44.1% at a 20% sampling rate). Similar trends are observed for CIFAR-10 and CIFAR-100, where SIA accuracy decreases with more clients (from 51% to 16% in CIFAR-10, and from 77% to 26% in CIFAR-100), but increases when only a subset of clients is sampled (up to 50.33% and 72.5%, respectively). This experiment highlights that SIAs can be generalized to settings with more clients, if subsampling is applied.

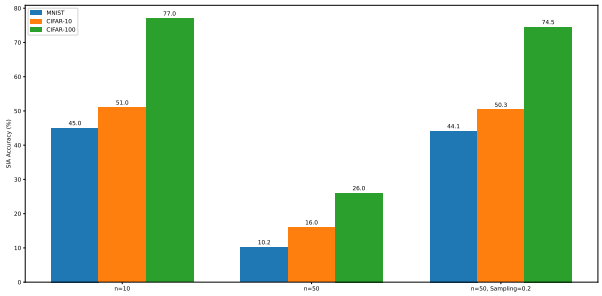

Figure 14: SIA accuracy on MNIST (blue), CIFAR-10 (orange) and CIFAR-100 (green) under client sampling with $\alpha = 0.1$ and 10 local epochs.